한국부식학회지
Journal of the Corrosion Science Society of Korea
Vol. 16, No. 3, Sept. 1987
〈研究論文〉

Initiation of Stress Corrosion Cracking of 26Cr-1Mo Ferritic Stainless Steels in Hot Chloride Solution

H. S. Kwon* and R. F. Hehemann**

*School of Mechanical & Materials Eng. Korea Institute of Technology
**Deceased, formerly professor in Dept. of Metallurgy and Materials Science at Case Western Reserve University, Cleveland, Ohio.

ABSTRACT

Elongation measurements of 26Cr-1Mo ferritic stainless steels undergoing stress corrosion in boiling LiCl solution allow the induction period to be distinguished from the propagation period of cracks by the deviation of elongation from the logarithmic creep law. Localised corrosion cells are activated exclusively at slip steps by loading and developed into corrosion trenches. No cracks have developed from the corrosion trenches until the induction period is exceeded. The induction period is regarded as a time for localised corrosion cells to achieve a critical degree of occlusion for crack initiation.

The repassivation rate of exposed metal by creep or emergence of slip steps decreases as the load increases and is very sensitive to the microstructural changes that affect slip step height. The greater susceptibility to stress corrosion cracking of either prestrained or grain coarsened 26Cr-1Mo alloy compared with that of mill annealed material results from a significant reduction of repassivation rate associated with the increased slip step height. The angular titanium carbonitrides particles dispersed in Ti-stabilized 26Cr-1Mo alloy have a detrimental effect on the resistance to stress corrosion cracking.

Introduction

The conventional ferritic stainless steels such as 430 have exhibited immunity in the same chloride environments that promote streee corrosion cracking (SCC) in the austenitic stainless steels[1]. This results largely from their inferior corrosion resistance resulting in failure by pitting and general corrosion rather than SCC[2]. The recently developed corrosion resistant grades containing 26 ~ 29% Cr and 1 ~ 4% Mo have proved a practical solution to many chloride SCC problems[2,3]. In general, these alloys are immune to chloride SCC under freely corroding conditions when tested in the mill annealed condition. However, susceptibility can be induced by compositional variations, particularly small

amounts of Cu or Ni, or by prior thermal and mechanical treatments [4,5]. For example, small amount of cold work or high temperature treatments that enlarge grain size induce failure at the corrosion potential, E_{oc}.

SCC of ferritic stainless steels occurs at potentials noble to a critical value that has been designated as the cracking potential, E_{cc}. The E_{cc} for the low interstitial high chromium alloys is very sensitive to prior thermal and mechanical treatments[5]. The microstructural changes induced by these treatments have an significant effects on slip, creep and repassivation behaviors that are very important variables in the initiation of SCC. The purpose of this research is to investigate the initiation process of SCC of high chromium ferritic stainless steels with evaluating the role of slip, creep and repassivation in the SCC reaction and to elucidate how these variables are influenced to induce susceptibility to SCC by prior thermal and mechanical treatments.

Materials and Experimental Procedures

The commercial alloys with the same base composition of 26Cr-1Mo were employed in this study. One was the low interstitial version, E-Brite (ASTM XM-27) and the other a high interstitial alloy designated as 26-1S (ASTM XM-33). The 26-1S is an alloy stabilized by titanium addition of approximately seven times its carbon and nitrogen content. These materials were provided by Allegheny Ludlum Steel Corp. in the form of annealed sheet 1.24mm thick. Chemical compositions of the alloys are presented in Talbe I.

Samples of E-Brite and 26-1S were annealed for one half hour at 1050°C and water quenched to study the effect of enlarged grain size on stress corrosion behavior. The influence of cold deformation on stress corrosion behavior was evaluated at 5% plastic tensile strain by prestraining mill annealed specimens. Grain size and yield strength of the alloys in the mill annealed, deformed and heat treated conditions are shown in Table 2.

SCC tests were conducted in uniaxial tension using the constant load type fixtures and environmental cell described previously[6]. Tensile specimens with a gage section of 50mm long and 3.5mm wide were used in SCC test. The elongation of the specimen due to creep and crack propagation during SCC test was recorded as a function of time by measuring beam deflection. Unless stated otherwise, SCC specimens were loaded to 90% of the yield strength.

All tests were performed in boiling 42% LiCl solution containing lgm Thiourea (NH_2CSNH_2) per 100gm LiCl as a hydrogen recombination poison at 140°C. All SCC tests were conducted in solution deaerated with nitrogen with loads and/or polarization applied after a stabilized corrosion potential had been achieved. All potentials are referred to the saturated calomel electrode (SCE).

Both the surface associated with film breakdown and the polished cross section of specimens were examined with a optical microscope to determine the mode and the extent of the localized attack. In order to observe slip steps produced during transient creep, polished samples were loaded in silicone oil at the temperature and stress employed in the SCC test. These slip steps were observed with a optical microscope.

Table 1. Chemical Composition of 26Cr-1Mo Alloys.

Alloy	Chemical Composition - Pct								
Designation	C	N	Cr	Mo	Ni	Ti	Cb	Mn	Si
E-Brite	0.001	0.010	26.1	0.99	0.13	0.037	0.085	0.02	0.31
26-1S	0.02	0.068	26*	1*	0.25	0.49	0.003	NA	NA

* Indicates nominal composition.

NA Indicates no intentional addition and not analyzed.

Table 2. Grain size and yield strength of 26Cr-1 Mo Alloys.

Alloy Designation	Prior Treatment	ASTM Grain Size	0.2% Offset Yield Strength (Ksi)
E-Brite	Mill Annealed	7/6	53.6
E-Brite	1050 C ½hr. -W.Q.*	2/1	50.2
E-Brite	5% Deformed	7/5	70.0
26-1S	Mill Annealed	8/7	54.8
26-1S	1050 C ½hr. -W.Q.	2/1	45.0
26-1S	5% Deformed	8/7	69.8

* Specimens were annealed for 1/2 hour in air at 1050°C and water quenched.

Results and Discussion

Cracking Susceptibility of 26Cr-1Mo Alloys

The susceptibility to SCC can be revealed by time to failure or critical cracking potential, E_{cc}. Time to failure put an emphasis on the reaction rate of SCC, whereas E_{cc} provides an electrochemical parameter determining whether or not SCC occurs for given conditions. Specifically, cracking does occur in metal/environment systems in which corrosion potential, E_{oc}, is noble to E_{cc}.

The influence of applied potential on time to failure was employed to identify cracking potentials. Figure 1 compares the susceptibility to cracking of E-Brite and 26-1S. Both steels exhibit the same corrosion potential, -500mV, however, their cracking potentials differ by more than 130mV. For 26-1S, E_{cc} is 125mV active to E_{oc} and failure does occur at open circuit. On the other hand E-Brite is immune to SCC at open circuit but became susceptible when anodically polarized exhibiting a cracking potential 15mV noble to the E_{oc}. This slight difference in the corrosion and cracking potentials of E-Brite suggests that only small variations in the structure of alloy may reverse the relationship between these potentials resulting in susceptibility. Indeed, microstructural changes by prior thermal and mechanical treatment modify the stress corrosion response of E-Brite but are essentially without effect on 26-1S. These data are compared in Table 3. For E-Brite, either 5% Prestrain or grain coarsening annealing treatments induced susceptibility to cracking by displacing E_{cc} in the active direction without changing E_{oc}.

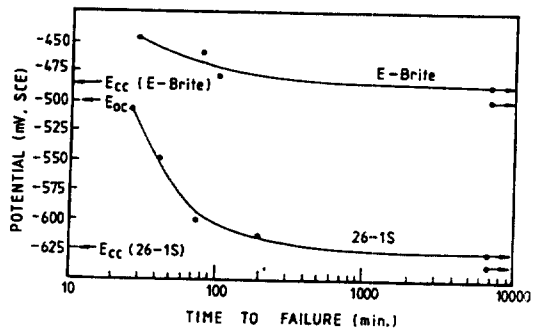

Fig. 1. Influence of applied potential on time failure of E-Brite and 26-1S respecitively loaded 90% of the yield strength in 42% LiCl+Thiourea at 140°C.

Table 3. Comparison of the Corrosion and Cracking Potentials of E- Brite and 26-1S in 42% LiCl+Thiourea at 140°C

Alloy	Condition	E_{oc} (mV, SCE)	E_{cc} (mV, SCE)	Difference
E-Brite	Mill Annealed	-500	-485	+15
E-Brite	5% Prestrain	-500	-570	-70
E-Brite	1050 C, ½hr., W.Q.	-500	-625	-125
26-1S	Mill Annealed	-500	-625	-125
26-1S	5% Prestrain	-500	-625	-125
26-1S	1050 C, ½hr., W.Q.	-500	-625	-125

The insensitivity of corrosion potential to the prior thermal and mechanical treatments and the minor compositional variations sussests that

E_{oc} of 26-Cr-1Mo steels is influenced by the properties of surface film rather than microstructural changes of the material. On the other hand, E_{cc} of E-Brite appears to be greatly influenced by the microstructural changes that have a great influence on the slip and repassivation behaviors.

Induction Period of SCC

Elongation of specimens undergoing stress corrosion were measured to identify the induction and propagation periods of crack, and also to evaluate the effects of creep on these periods. Figure 2 shows a typical elongation (or extension)-time curve for mill annealed E-Brite polarized to a potential of -460mV noble to E_{cc} in boiling 42% LiCl plus Thiourea. It is evident that the elongation initially obeys a logarithmic creep law such as

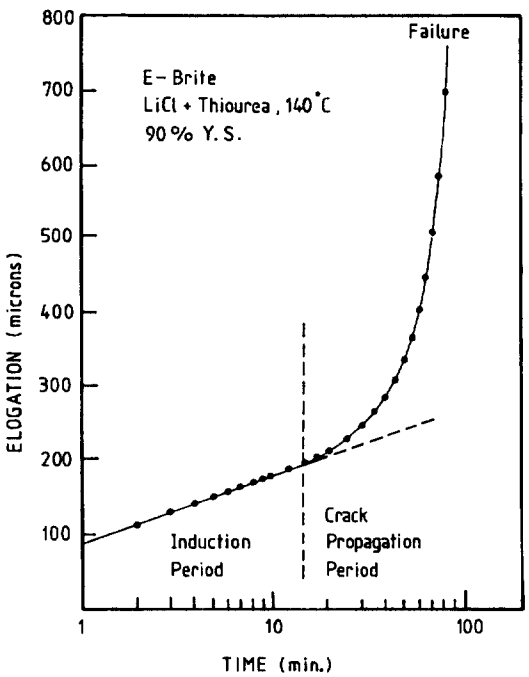

Fig. 2. Elongation as a function of time for mill annealed E-Brite stressed 90% of the yield strength and anodically polarized to -460mV in boiling 42% LiCl+Thiourea.

$$L(t) = L_1 + \alpha \log(t)$$

Where L(t) is the elongation at time t, and L_1 is the elongation measured during first one minute, t is in minutes.

The transition from the induction period to the propagation period is revealed by deviation of the elongation-time curve from the logarithmic creep law. The slope(α) in Figure 2 corresponded to that obtained from the creep curve of mill annealed E-Brite in an inert environment using silicone oil at the same temperature and stress employed in the SCC test. This indicates that the elongation during the induction period is not influenced by environmental attack but results simply from transient creep. However this does not mean that localized corrosion are not occurring during the induction period. Specifically, corrosion trenches were observed on the sample removed from the environment during the induction period as shown in Figure 3. No cracks, however, had developed from the trenches during the induction period. The growth of cracks from the bottom of corrosion trenches did occur after the elongation-time relationship had diverged from the lograrithmic creep law. The cracks then propagated to failure at an increasing rate.

Formation of Corrosion Trenches

The formation of corrosion trenches during the induction period results from the localized corrosion that is associated with breakdown of a protective surface film. It is well established[7,8] that slip induced film rupture can lead to SCC of austenitic stainless steel well below the yield strength. However, stress corrosion cracks in austenitic stainless steels have frequently been reported to initiate from preexisting pits[9]. E-Brite appears to be highly resistant to localized

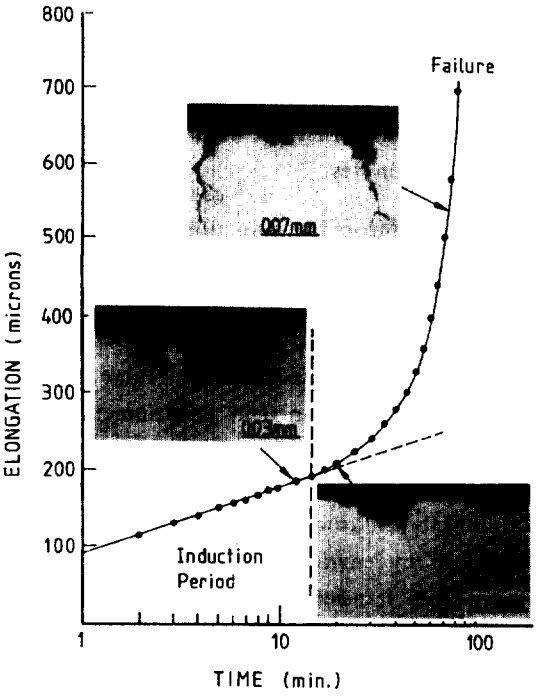

Fig. 3. Cross sectional metallographs of mill annealed E-Brite stressed 90% of the yield strength in boiling 42% LiCl+Thiourea at -460mV. Each metallograph was obtained from the specimen that was removed from the environment at the stage indicated by an arrow on the elongation-time curve.

corrosion. Samples of E-Brite exposed for 2 days to boiling 42% LiCl plus Thiourea did not reveal any occurrence of localized corrosion. This shows that the protective film of E-Brite is essentially free of defects capable of functioning as sites for the chemical breakdown of the film under freely corroding conditions. Thus, film rupture by creep or emergence of slip steps will be an alternative, mechanical means for initiating localized corrosion that takes the form of corrosion trenches. Figure 4 demonstrates clearly that localized corrosion of E-Brite initiates exclusively at the slip steps. Most of slip steps shown in Figure 4 are developed during the initial application of the load, and these continue to evolve with time so that they are effective in the formation of the corrosion trench.

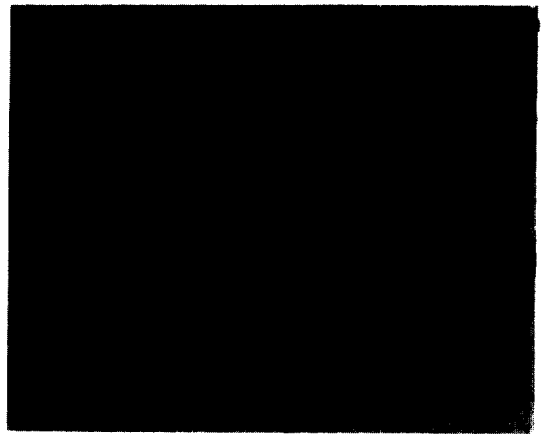

Fig. 4. Initial corrosion attack of mill annealed E-Brite stressed for 15 seconds to 90% of the yield strength in boing 42% LiCl+Thiourea at 140℃

The film rupture in stainless steels leads to the development of an occluded cell accompanied by the well known acidification and concentration of chloride ion[10]. The acidification, arising from the hydrolysis of chromic and other cations produced by anodic dissolution of metals, results in depassivation when a critical pH or combination of pH and Cl^- ion concentration is achieved in the occluded cell[11]. The maintenance of a critical value of pH and Cl^- ion concentration is required for pit growth[12] or crack propagation[13];[14]. As the degree of occlusion of corrosion trenches increases due to the anodic dissolution of metal at active sites, acidity and concentration of Cl^- ion will attain a critical value at which cracks can be initiated. Therefore, the induction period is regarded as a time for the localised corrosion cell to achieve a critical degree of occlusion, thereby maintaining the pH and Cl^- ion concentration required for the crack initiation and propagation.

The induction periods of SCC are also clearly identified on the elongation-time curves for grain coarsened or 5% prestrained E-Brite and 26-

1S. The induction periods for these materials are influenced by applied stress, potential and prior thermal and mechanical treatments since these variables affect the creep and repassivation rates that control the amount of anodic dissolution of metal for the formation of corrosion trench.

The influence of stress on the induction and propagation periods is indicated in Table 4. As expected, a reduction of the applied stress from 90% to 80% of the yield strength in mill annealed E-Brite at -460mV increases the time to failure. This increase in the time to failure resulted primarily from an increased induction period with a lesser effect on the propagation period. In other words, the formation of trench with a critical degree of occlusion is a stress dependent process, whereas propagation of cracks appears to be less stress dependent. This behavior in ferritic stainless steel parallels that in austenitic stainlesss steel[15]. The short induction time for mill annealed E-Brite stressed to 120% of the yield strength at open circuit in Table 4 can be attributed to its high creep rate. On the other hand, the increase in the induction period for mill annealed E-Brite stressed to 80% of the yield strength at -460mV results from the low rate of creep as shown in Figure 5. Applied potential also influences the induction period. Data in Table 5 shows that the displacement of applied potential in the active direction from -460mV to -480mV increase the induction period of mill annealed E-Brite from 15min. to 32min. This arises from the fact that the dissolution rate of metal at active sites increases with increasing potential in the noble direction.

The induction period of E-Brite measured at 90% of the yield strength is very sensitive to the prior thermal and mechanical treatment as indicated in Table 4. The induction period of either 5% deformed or grain coarsened material is shorter than that of mill annealed material in spite of their comparable or even lower creep rates. This is explained in detail by the effect of the slip step height on the overall repassivation rate in next section.

Table 4. Influence of Stress on Time to Failure of E-Brite in Boiling 42% LiCl+Thiourea

Material Condition	Potential (mV,SCE)	Applied Stress (% of Y.S.)	Logarithmic Creep Rate (Microns/ Log (Min.)	Time To Failure (Min.)	Induction Period (Min.)	Propagation Period (Min.)
Mill Annealed	-460	75	35	N.F.(1) (7200)	-	-
Mill Annealed	-460	80	45	140	75	65
Mill Annealed	-460	90	80	82	15	67
Mill Annealed	O.C.(2)	110	110	N.F.(7200)	-	-
Mill Annealed	O.C.	120	145	28	10	18
Grain Coarsened	O.C.	90	55	35	13	22
5% Prestrained	O.C.	90	88	28	12	16

(1) N.F. = no failure

(2) O.C. = open circuit

Table 5. Influence of Potential on Time to Failure of Mill Annealed 26Cr-1Mo Alloys in 42% LiCl+Thiourea at 90% of the Yield Strength.

Alloy Designation	Applied Potential (mV, SCE)	Logarithmic Creep Rate (Microns/Log (Min.))	Time To Failure (Min.)	Induction Period (Min.)	Propagation Period (Min.)
E-Brite	-460	80	82	15	67
E-Brite	-480	80	98	32	66
E-Brite	-500	80	N.F.(7200)	-	-
26-1S	O.C.	70	56	23	33
26-1S	-600	70	72	40	32
26-1S	-625	70	N.F.(7200)	-	-

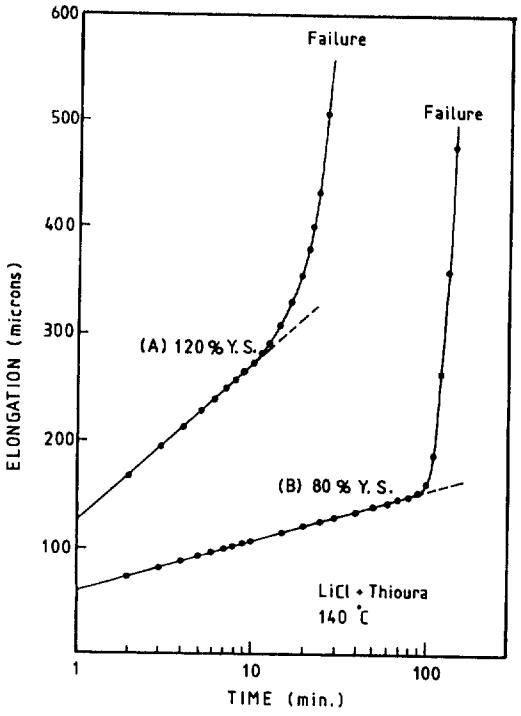

Fig. 5. Elongation-time curve for mill annealed E-Brite in boiling 42% LiCl+Thiourea, Showing effect of stresses on the crack initiation periods.
(A) Loaded 120% of the yield strength.
(B) Loaded 80% of the yield strength and anodically polarized to -460mV.

Film Rupture and Repassivation

As discussed in previous section, localised corrosion cells activated by creep or emergence of slip steps during loading cannot initiate cracking until a critical degree of occlusion has developed. This requires an appropriate balance of the inherent rate of repassivation of unfilmed surface and the rate of exposure of this surface by creep or emergence of slip steps [7,15; 16]. The inherent rate of repassivation of unfilmed surface depends on potential; however, for a given potential, the rate of exposure of new surface by creep or emergence of slip steps controls the overall rate of repassivation. Thus, either potential-time curves determined at open circuit or current time curves for polarized samples reveal the effects of applied stress and structural changes by either the intersitial content or the prior thermal and mechanical treatment on the overall repassivation rate.

Figure 6 illustrates the substantial difference in overall repassivation rates produced by creep under sustained load compared with that which occurs when the load is removed immedi-

ately after its application. Film rupture during loading produces an immediate displacement of corrosion potential in the active direction. The rate of repassivation under substained load is substantially reduced compared with that observed by immediate removal of the load. The overall repassivation rate decreases as the sustained load is increased. This difference in repassivation rate is attributed to the continued exposure of unfilmed metal by creep and reduction of the load provides intermediate values of the repassivation rate. For mill annealed E-Brite, complete repassivation occurs at stress of 90% of the yield strength thereby preventing crack initiation under open circuit condition. The repassivation rate must be reduced by anodic polarization in order for cracking to occur.

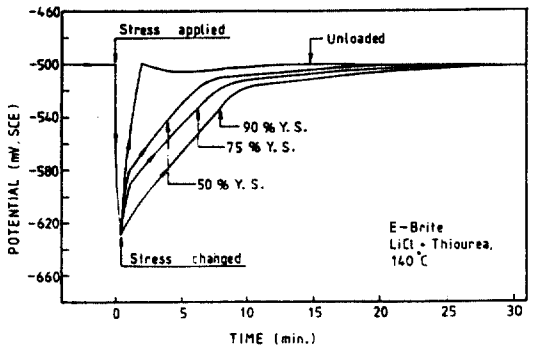

Fig. 6. Effect of stress change on repassivation revealed by corrosion potential-time curve for mill annealed E-Brite initially stressed to 90% of the yield strength in 42% LiCl+Thiourea at 140℃.

In similar tests, the repassivation rate of mill annealed 26-1S that occurs when the load is removed immediatly after its application is almost the same as that of mill annealed E-Brite. However, under equivalent loads, the repassivation rate of mill annealed 26-1S is slower than that of mill annealed E-Brite as illustrated in Figure 7. This difference in repassivation rate between E-Brite and 26-1S is more pronounced at higher sustained loads and appears to arise from a difference in their deformation response rather than a difference in the inherent repassivation rate between them. 26-1S, being stabilized with titanium, contains massive titanium carbonitride particles. These angular particles may produce regions of high stress concentration during loading and function as a dislocation source. Further, the difference in thermal expansion coefficient and elastic constants between titanium carbonitrides and the matrix may provide a crevice around these particles upon loading or quenching. Indeed, localized corrosion occurred exclusively around titanium carbonitrides on unstressed sample of 26-1S exposed for 2 days to boiling 42% LiCl+Thiourea solution. The titanium carbonitrides as susceptible sites for film breakdown provide one of the reasons why 26-1S is more susceptible to stress corrosion cracking than is E-Brite. Repassivation of mill annealed 26-1S at 90% of the yield strength took place sufficiently slowly that failure occurred (Figure 7). Whereas, for mll annealed 26-1S loaded 75% of the yield strength or below, complete repressivation occurs thereby preventing crack initiation.

Repressivation of grain coarsend E-Brite occurred at a greatly reduced rate resulting in

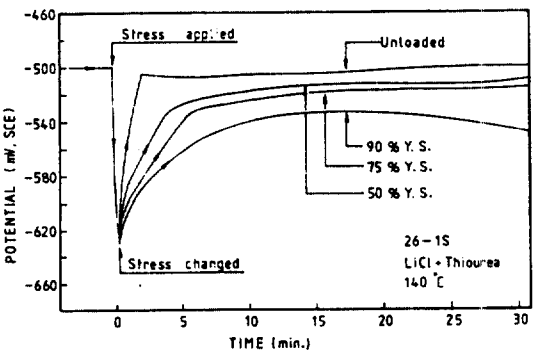

Fig. 7. Effect of stress change on repassivation behavior revealed by corrosion potential-time curve for mill annealed 26-1S initially stressed to 90% of the yield strength in 42% LiCl+Thiourea at 140℃.

crack initiation and propagation to failure under open circuit conditions as shown in Figure 8. The potential-time response of 5% prestrained E-Brite is similiar to that of the grain coarsened material. These reduced repassivation rates of grain coarsened or 5% prestrained material result not from high creep rate (Table 4) but from increased slip step height as shown in Table 6[17]. Once film rupture has occurred, it is the continued evolution of slip step that controls the repassivation rate and the slip step height is a result of the continued evolution of slip step during loading. The increased slip step height is very effective in decreasing both the repassivation rate and the induction period since the amount of

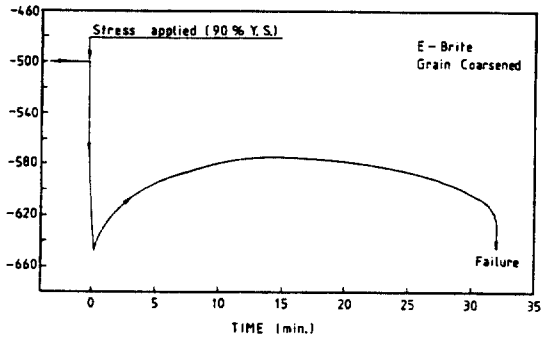

Fig. 8. Corrosion potenital-time behavior of grain coarsened E-Brite upon loading of 90% of the yield strength in 42% LiCl+Thiourea at 140℃.

Table 6. Slip Step Height of E-Brite Specimens Stressed 90% of the Yield Strength for One Hour in Silicone Oil at 140°C

Material Condition	Height (nm)
Mill annealed	40
Grain Coarsened	117
5 pct prestrained	210
Prestrained + 3 Hour annealing at 250°C	80

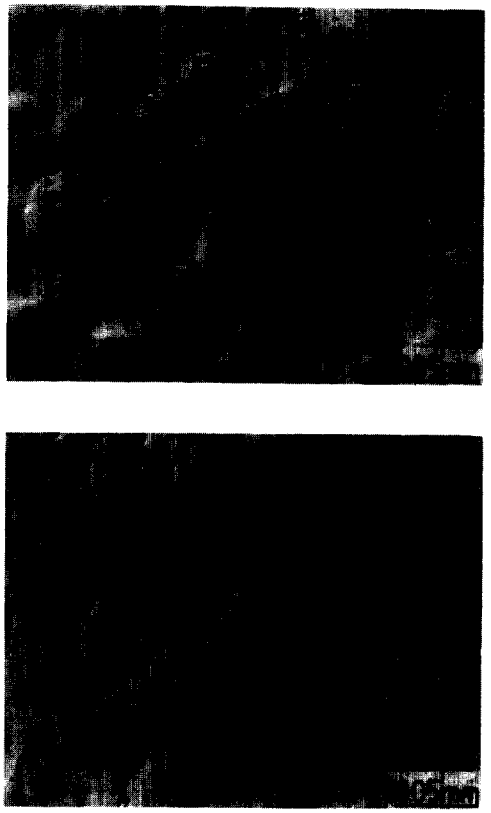

Fig. 9. Sip steps formed on the surface of E-Brite stresed for 1 hour in silicone oil at 140℃. (A) mill annealed E-Brite. (B) 5% prestrained B E-Brite.

metal dissolution is proportional to the unfilmed area. Figure 9 shows that slip steps formed on prestrained E-Brite are coarser than those on mill annealed material. For grain coarsened E-Brite, the increased slip step height results from its large grain size. It was demonstrated[18] that the number of dislocations moving out of the surface to form a slip step is proportional to the grain size. Thus the larger the grain size, the greater the slip step height, and the higher the susceptibility to SCC. For the prestrained E-brite, an increased slip step height presumably results from the generation of dislocations and dislocation sources by the deformation process. The susceptibility to SCC of E-Brite induced by prestrain can be

ameliorated by low temperature annealing treatment at 250°C[5]. This is cosistent with the immobilization of dislocations generated during prestrain by pinning with carbon and nitrogen. Indeed, increased slip step height of prestrained material returned toward that of mill annealed material (Table 6) restoring the more rapid repassivation rate for preventing crack initiation.

The cathodic polarization reduce the effect of the increased slip step height on the overall repassivation rate by increasing the inherent repassivation rate. Thus, the critical cracking potential for either prestrained or grain coarsened E-Brite must be shifted in the active direction relative to the corrosion potential as indicated in Table 3.

Conclusions

1. The cracking potentials of 26Cr-1Mo stainless steels are very sensitive to the prior thermal and mechamical treatments and the minor compositional variations. Either 5% prestrain or a grain coarsening annealing treatment induces susceptibility to SCC of the low interstitial alloy by displacing its cracking potential in the active direction without changing the corrosion potential. The high interstitial alloy, on the other hand, exhibits a cracking potential that is insensitive to prestraining or grain coarsening treatments.
2. Elongation-time curves of 26Cr-1Mo stainless steels undergoing stress corrosion exhibit clearly the induction and propagation periods of cracks. Localised corrosion cells are activated exclusively at slip steps by loading and developed into corrosion trenches. No cracks had developed from the corrosion treches during the inducion period. The induction period is regarded as a time for localised corrosion cells to achieve a critical degree of occlusion for crack initiation.
3. The repassivation rate of exposed metal by creep or emergence of slip steps decreases as the sustained load increases and is very sensitive to the microstructural changes that affect slip step height. The greater susceptibility to SCC of either prestrained or grain coarsened E-Brite compared with that of mill annealed material results from a significant reduction of repassivation rate associated with the increased slip step height.
4. The angular titanium carbonitride particles dispersed in Ti-stabilized 26Cr-1Mo alloy provide favorable sites for localised corrosion to occur. This is the reason why Ti-stabilized 26Cr-1Mo alloy is more susceptible to SCC than is the low interstitial alloy.

References

1. M. A. Sheil : ASTM-AIME Symposium on stress corrosion cracking of metals, 1944, ASTM, 395 (1945)
2. R. F. Steigerwald et al : Corrosion *33*, 270 (1977)
3. M. A. Streicher : "Conf. Stainless steel 77" Sponsored by Climax Molybdenum Co., 121 (1978)
4. A. P. Bond and H. J. Dundas : Stress Corrosion Cracking and Hydrogen Embrittlement of Iron Base Alloys, R. W. Staehle et al eds. NACE-5, 1136 (1977)
5. T. E. Mohr, A. R. Troiano and R. F. Hehemann : Corrosion, *33*, 199 (1981)
6. M. Smialowski and M. Rychik, Corrosion, *23*, 218 (1967)
7. J. C. Scully : The theory of stress corrosion cracking of alloys, J. C. Scully ed., NATO. 1 (1971)

8. R. W. Staehle : Ref 7, 223
9. Z. Szklarska smialowska and N. Lukomoski: Corrosion, *34*, 177 (1978)
10. P. R. Rhodes : Corrosion, *25*, 462 (1969)
11. H. Ogawa, et al. : Tetsu-to-Hagane, *63*, 605 (1979)
12. Z. Szklarska Smialowska and J. Mankowski: Corrosion Sci., *12*, 925 (1972)
13. M. Marek and R. F. Hochman : Corrosion, *26*, 5 (1970)
14. J. C. Scully : Corrosion Sci., *26*, 997 (1980)
15. M. C. Petit and D. Desjardins : Ref. 4, 1205
16. D. A. Vermilyea : Ref. 4, 208 (1977)
17. R. Iyer : Ph. D Thesis, Case Western Reserve University, Cleveland, OH, 1985
18. T. J. Smith and R. W. Staehle : Corrosion, *23*, 117 (1967)